arXiv:1605.07637v1 [cond-mat.quant-gas] 24 May 2016

Many-Body Quantum Optics with Decaying Atomic Spin States: (γ, κ) Dicke model

Jan Gelhausen,* Michael Buchhold,† and Philipp Strack‡

Institut für Theoretische Physik, Universität zu Köln, D-50937 Cologne, Germany

(Dated: March 20, 2024)

Abstract

We provide a theory for quantum-optical realizations of the open Dicke model with internal, atomic spin states subject to uncorrelated, single-site spontaneous emission with rate γ. This introduces a second decay channel for excitations to irreversibly dissipate into the environment, in addition to the photon loss with rate κ. We compute the mean-field non-equilibrium steady states for spin and photon observables in the long-time limit, $t \to \infty$. Although γ does not conserve the total angular momentum of the spin array, we argue that our solution is exact in the thermodynamic limit, for the number of atoms $N \to \infty$. In light of recent and upcoming experiments realizing superradiant phase transitions using internal atomic states with pinned atoms in optical lattices, our work lays the foundation for the pursuit of a new class of open quantum magnets coupled to quantum light.

* jg@thp.uni-koeln.de

† buchhold@thp.uni-koeln.de

‡ strack@thp.uni-koeln.de; http://www.thp.uni-koeln.de/~strack/

CONTENTS

I. Introduction 2

A. Key results and outline of paper 4

II. (γ, κ) Dicke model 4

A. Hamiltonian and Liouvillians 4

B. Symmetries 6

C. Exact solvability in long-time limit $t \to \infty$ and thermodynamic limit $N \to \infty$ 6

D. Experimental context in cavity QED 7

E. Heisenberg-Langevin equations 8

III. Results 9

A. Critical coupling for onset of superradiance $g_c(\kappa, \gamma)$ 10

B. Comparison with Singapore experiment 11

C. Non-equilibrium steady states for spins and photons 13

D. Cavity output spectrum 15

E. Effective temperature 17

IV. Conclusions 19

Acknowledgments 19

A. Details of calculation for cavity spectrum 20

B. Details of calculation for effective temperature 21

References 22

I. INTRODUCTION

Significant research efforts in the science of quantum optics are directed towards "scaling up" the minimal building block of one atomic qubit and one single photon towards N qubits and M photons. One objective is that a controllable assembly of such systems in the quantum regime has all the ingredients of a quantum computer including channels for communication of information

within quantum networks [1]. This development represents both, a tremendous opportunity and a challenge, to seriously study the many-body physics of extended quantum-optical systems, where arrays of qubits are coherently coupled to quantum light.

To that end, a promising recent experimental development is the realization of tunable lattice potentials within resonators hosting photons with optical wavelengths [2–4]. These set-ups allow controllable placement of large numbers of quantum emitters, in the form of ultracold atoms, into lattice sites, preserving their relative phases. The atom-cavity coupling now has "single-site resolution" by overlaying cavity mode functions with lattice potentials and the targeted loading process of atoms into given lattice sites.

Making the lattice potentials sufficiently deep, one can now access a regime in which the atomic motion is suppressed completely and the dynamics of *internal, spin excitations* play the lead role. Although the analogy is dangerous and incomplete, let us mention that a corresponding situation in an electronic condensed matter material would be a Mott insulator, in which the charge degrees of freedom are localized, and the electronic spins interact via, typically short-ranged, exchange couplings J_{ij}. As was recognized theoretically a few years back, the cavity set-up allows a much richer set of $J_{\ell m}$'s (variable range, complex- vs. real-valued) and unconventional magnetic phases to be realized [5–7]. However, the "drosophila" in this field is the Dicke model, an infinite-ranged, exactly solvable ferromagnet [8, 9], which has recently also been realized experimentally using internal spin states [10, 11].

A basic physical difference to the earlier realizations of the Dicke model using *momentum states* of a thermal or condensed Bose gas [12, 13] is the increased fragility of internal, spin states to dissipative processes such as atomic spontaneous emission. Indeed, the decay rate of collective momentum modes $\gamma_{\rm mom}$ of an atomic gas is remarkably small ($\gamma_{\rm mom} \ll \kappa \lesssim g$) and limited mostly by thermal effects and collisions [14–18]. By contrast single-site atomic spontaneous emission with rate γ tends to deplete the system of excitations and driving each spin into the $|\downarrow\rangle$ state. There is no analog of this dissipative process for momentum states and therefore its basic physical effects have not been explored much in this context. Moreover, the experiments by Baden *et al.* [11] were not entirely able to compare their data to a theory for the open Dicke model with spontaneous emission, clearly identifying a gap in the current literature.

The objective of this paper to reveal the interplay of single-site spontaneous emission with the collective interactions induced by the resonator. We extend previous works of the open Dicke model [10], which were restricted to photon losses, to the full two loss channels (γ, κ) variant. By

this, we want to lay the foundation for the study of interacting, open quantum magnets with atoms in optical lattices in many-body cavity QED [2–4] and other nano-photonic setups such as atoms trapped to close to photonic crystals [19, 20].

A. Key results and outline of paper

Our main result is the derivation of the exact formula of the critical coupling for the onset of superradiance in Sec. III A in the presence of atomic spontaneous emission. In Sec. III B, we then use this result to resolve an observed discrepancy between experimental data for the critical pump strength and earlier calculations. The argument why this formula remains exact in the presence of single-site γ, is given in Sec. III B. In short, site-to-site variances between observables vanish in the thermodynamic limit, because the Hamiltonian affects only the homogeneous, zero-momentum component of the spins. It is true that γ also couples to finite-k components, in constrast to the κ-only Dicke model, but γ just leads to their decay.

Based on the Heisenberg-Langevin equations compiled in Sec. II E, we complete the program and also compute the values of non-equilibrium steady states, the cavity output spectrum, and the effective temperature of the photons in Sec. III C-III E.

II. (γ, κ) DICKE MODEL

In this section, we begin by explaining the model Dicke Hamiltonian and the Liouvillians for the two decay processes: photon loss and atomic spontaneous emission. Then, we connect this model to a recent quantum optics experiment, wherein the spin states in the Dicke Hamiltonian were realized via two atomic hyperfine-split levels. We finally present the Heisenberg-Langevin equations within the Markov approximation.

A. Hamiltonian and Liouvillians

The core of the set-up is an array of N atomic spins at fixed positions in space. These spins are subject two to types of dynamical processes. The first is coherent and reversible conversion into photonic excitations via an homogeneous atom-photon coupling g. This is in accordance with probability-preserving rules of unitary quantum mechanics and can be described by the Hamilto-

nian

$$H = \omega_0 a^\dagger a + \left(\frac{U}{2N}\sum_{\ell=1}^{N}\sigma_\ell^z\right)a^\dagger a + \frac{\Delta}{2}\sum_{\ell=1}^{N}\sigma_\ell^z + \frac{g}{\sqrt{N}}(a+a^\dagger)\sum_{\ell=1}^{N}(\sigma_\ell^+ + \sigma_\ell^-)\,, \tag{1}$$

where there is also an (effective) photon energy ω_0, a longitudinal field in z-direction for the spins Δ, and an additional frequency shift of the photons due to a coupling U to the collective z-component. This last coupling arises in the quantum-optical implementation we discuss below in Subsec. II D.

The second class of processes introduce decoherence and are irreversible decay processes of both, photonic (rate κ) and atomic excitations (rate γ) into the reservoir modes of the electromagnetic vacuum surrounding the cavity. Their effect can be captured by introducing the Lindblad operators, which act on the system density matrix ρ in the following way:

$$\mathcal{L}_\gamma[\rho] = \frac{\gamma}{2}\sum_{\ell=1}^{N}\Big[2\sigma_\ell^-\rho\sigma_\ell^+ - \{\sigma_\ell^+\sigma_\ell^-,\rho\}\Big], \tag{2}$$

$$\mathcal{L}_\kappa[\rho] = \kappa\Big[2a\rho a^\dagger - \{a^\dagger a,\rho\}\Big]\,. \tag{3}$$

Here the atomic spontaneous emission acts on each atom on site ℓ independently. In quantum optics, the reservoirs have Markovian character; this is because the Hamiltonian Eq. (1) becomes time-independent only in a frame rotating with an optical (pump) frequency. In this frame, bath and system times scales are well separated by different orders of magnitude.

The interplay and competition between unitary and irreversible dynamics can be studied with a Master equation for the density matrix

$$\dot\rho = -i[H,\rho] + \mathcal{L}_\kappa[\rho] + \mathcal{L}_\gamma[\rho]\,. \tag{4}$$

A key property of $\mathcal{L}_\gamma$ is that, in general, it cannot be written in terms of a collective spin operator, as spin decay events are uncorrelated between sites. Its very basic physical effect is to deplete the system of atomic excitations, that is, incoherently drive each spin into the $|\downarrow\rangle$ state. As the Hamiltonian in Eq. (1) does not conserve the total number of excitations $\mathcal{N} = a^\dagger a + \frac{1}{2}\sum_{\ell=1}^{N}\sigma_\ell^z + \frac{N}{2}$ the Hamiltonian will counteract the depletion processes of the Lindblad terms. This is in contrast to a Hamiltonian where the counter-rotating terms are dropped in an rotating-wave-approximation and for which there would be no other steady-state as the empty dark-state. One should note that in the presence of spontaneous atomic decay $\gamma \neq 0$, the case of $\Delta < 0$ displays no interesting low-energy physics, i.e. no superradiance transition is present, since the system is pumped towards a high energy state in this case.

B. Symmetries

Eq. (4) is invariant under a combined, discrete $\mathbb{Z}_2$ symmetry transformation

$$\mathbb{Z}_2 : [a + a^\dagger, \sigma_\ell^x, \sigma_\ell^y] \to [-(a + a^\dagger), -\sigma_\ell^x, -\sigma_\ell^y)], \tag{5}$$

which corresponds to a unitary transformation

$$U_\pi = \exp(i\pi \left(a^\dagger a + \sum_{\ell=1}^{N} \sigma_\ell^z \right)). \tag{6}$$

This symmetry is spontaneously broken at the superradiant Dicke transition.

Additionally, the spin sector of the Hamiltonian in Eq. (1) is invariant under a combination of time reversal $\mathcal{T}_\ell = -i\sigma_\ell^y K_\ell,\ t \to -t$ (for a spin $s = 1/2$) and rotation in spin-space around the y-axis with angle $\theta = \pi$ denoted as $D_{y,\pi}^{1/2,\ell} = -i\sigma_\ell^y$, where K_ℓ is the complex conjugation operator such that $\mathcal{G}_\ell = D_{y,\pi}^{1/2,\ell}\mathcal{T}_\ell = -K_\ell$ and $\mathcal{G}_\ell\mathcal{G}_\ell^{-1} = 1$ with $[\mathcal{G}_\ell, \mathcal{G}_m^{-1}] = 0$ and $[\mathcal{G}_\ell, \mathcal{G}_m] = 0$. If we write $G = \Pi_{\ell=1}^N \mathcal{G}_\ell$ we have

$$GHG^{-1} = H. \tag{7}$$

In the absence of a loss channel in the spin sector, this means that the steady state must be invariant under this transformation as well, which enforces $\langle\sigma^y\rangle = \langle G\sigma^y G^{-1}\rangle = -\langle\sigma^y\rangle \stackrel{!}{=} 0$. This symmetry is broken in the presence of Liouvillian $\mathcal{L}_\gamma$ in the spin sector and therefore steady states with non-zero $\langle\sigma^y\rangle \neq 0$ are accessible in the dynamics. In the photon sector, the corresponding symmetry is broken as well due to the presence of $\mathcal{L}_\kappa$, which leads to complex expectation values $\langle a\rangle \in \mathbb{C}$.

We mention here that the Hamiltonian dynamics together with the Lindblad contribution $\mathcal{L}_\kappa$ conserves the pseudo-angular momentum $\langle \boldsymbol{S}(t)\rangle^2$ but this conservation is explicitly broken by $\mathcal{L}_\gamma$. Using semi-classical steady states defined below, one finds

$$\partial_t \langle \boldsymbol{S}(t)\rangle^2 = 2\langle \boldsymbol{S}(t)\rangle \cdot \partial_t \langle \boldsymbol{S}(t)\rangle = -\gamma\left(\langle \boldsymbol{S}(t)\rangle^2 + 2\langle\sigma^z(t)\rangle\left(1 + \frac{\langle\sigma^z(t)\rangle}{2}\right)\right), \tag{8}$$

such that the steady-state value requires $\lim_{t\to\infty}\langle \boldsymbol{S}(t)\rangle^2 = -2\langle\sigma^z\rangle\left(1 + \frac{\langle\sigma^z\rangle}{2}\right)$ to hold.

C. Exact solvability in long-time limit $t \to \infty$ and thermodynamic limit $N \to \infty$

It is known that the Dicke model in thermodynamic equilibrium is exactly solvable by a mean-field ansatz [8, 9]. Although the exact solutions get more complicated, this remains true for the

non-equilibrium steady states of atomic quantum gases in optical cavities [15, 18] provided one takes first the thermodynamic limit, number of atoms $N \to \infty$, and then the long time limit, $t \to \infty$ ("$t - N$ limit"). Now one may wonder whether this remains true given that single-site γ violates the conservation of total angular momentum of the spins.

Here we present a brief argument, which shows that mean-field non-equilibrium steady states solve Eqs. (1-4) exactly in the $t - N$ limit. To see that, first integrate out the photons. This can be done exactly retaining photon losses and other pump and loss terms for the photons as long as they are quadratic in the photon fields [21]. This yields a ferromagnetic all-to-all coupling $-J\left(\sum_{\ell=1}^{N}\sigma_\ell^x\right)\left(\sum_{m=1}^{N}\sigma_m^x\right)$ mediated by photon exchange. We may set $U = 0$ in Eq. (1). We now go the thermodynamic limit $N \to \infty$ and write the Hamiltonian in momentum-space. Momenta k are now continuous variables and integrated over $\int_k$ the appropriate Brillouin zones

$$H_{\text{eff}} = \frac{\Delta}{2}\int_k \delta_{k,0}\,\sigma_k^z - J\int_k \delta_{k,0}\,\sigma_k^x\sigma_{-k}^x\,. \tag{9}$$

The remaining Lindblad operator for γ reads in momentum space

$$\begin{aligned}\mathcal{L}_\gamma[\rho] &= \frac{\gamma}{2}\int_k\left[2\sigma_k^-\rho\sigma_k^+ - \{\sigma_k^+\sigma_k^-,\rho\}\right]\\ &= \frac{\gamma}{2}\int_k \delta_{k,0}\left[2\sigma_k^-\rho\sigma_k^+ - \{\sigma_k^+\sigma_k^-,\rho\}\right] + \frac{\gamma}{2}\int_{k\neq 0}\left[2\sigma_k^-\rho\sigma_k^+ - \{\sigma_k^+\sigma_k^-,\rho\}\right],\end{aligned} \tag{10}$$

where in the second line we have split off the decay for the zero-momentum component from the finite momentum components. Next observe that the Hamiltonian dynamics Eq. (9) operates strictly within only the zero-momentum sub-space of the spins (in position space this is the homogeneous component). So does the first Lindbladian term in the second line of Eq. (10). Therefore the zero-momentum component experiences a non-trivial competition of Hamiltonian and dissipative dynamics. The finite-k components do nothing but decay. In particular, there is *nothing in the Hamiltonian or Lindbladian that can change the momentum of a given state*. Therefore, in the long-time limit $t \to \infty$, it is legal to focus on the zero-momentum component, that is, the mean-field non-equilibrium steady states are actually the exact solution.

D. Experimental context in cavity QED

To realize Eq. (1) in an optical cavity system, it is advantageous to suppress the motion of the atoms sufficiently such that the internal spin state dynamics dominates. To that end, an additional

optical lattice potential inside the resonator has been realized recently by three different groups [2–4] paving the way for many-body quantum optics in which the relative phases of the emitters play a role. For the simple Dicke model the lattice and cavity mode function are engineered such that every atom couples with the same strength to the cavity photon. Other arrangements, including mutually incommensurate periods [22], can now be turned into experimental reality.

Moreover, some form of Raman-transition assisted pumping scheme is required to reach the strong-coupling regime for the effective spin-photon coupling g needed to achieve the Dicke transition [10, 11]. There, the atomic levels to realize an effective spin system can be the hyperfine-structure manifold of the ground states of ^{87}Rb. Typically this is the $5^2S_{1/2}$ state split into the $F = 1$ and the $F = 2$ manifold such that $|g\rangle = |\downarrow\rangle = |F = 1, m_F = -1\rangle$ and $|e\rangle = |\uparrow\rangle = |F = 2, m_F = -2\rangle$ are possible choices. Where e labels the effective excited state and g labels the effective ground-state. The hyperfine structure splitting in the ground state manifold is $\omega_1 = 2\pi \times 6.835$ GHz. The cavity-assisted Raman transitions are achieved by coupling to the first excited state manifold that is split into a fine-structure $5^2P_{1/2}$ with $F = 2$ and $F = 1$ that for this choice is on the order of 812 MHz. The external driving lasers are separated by approximately twice the ground-state hyperfine splitting such that the longitudinal field for the spins $\Delta \sim$ MHz. Moreover, the choice of laser frequencies in the experiment by Baden *et al.* [11] leads to the $\frac{U}{2}\left(\sum_{\ell=1}^{N}\sigma_\ell^z\right)a^\dagger a$ term in Eq. (1) and we will come back to this experiment below in Subsec. III B.

E. Heisenberg-Langevin equations

As we argued above, we may proceed by projecting the Master equation onto the homogeneous component. All sites will behave the same so we do not keep track of all the spatial indices but write the equations for a single representative site. The photon mode couples to all atoms with the same coupling constant g. The Heisenberg equation of motion for an arbitrary system operator A where A can be any operator from the set $(\sigma_i^+, \sigma_i^-, \sigma_i^z, a, a^\dagger)$, is calculated according to

$$\partial_t A = -i[A, H] + \frac{\gamma}{2}\sum_{\ell=1}^{N}\left(2\sigma_\ell^+ A\sigma_\ell^- - \{A, \sigma_\ell^+\sigma_\ell^-\}\right) + \kappa\left(2a^\dagger A a - \{A, a^\dagger a\}\right), \tag{11}$$

where the Hamiltonian is given by Eq. (1) and (κ, γ) refer to the cavity damping and the rate of spontaneous emission, respectively. For the atomic degrees of freedom we use the notation $\sigma_i^+ = |e\rangle_i\langle g|, \sigma_i^z = |e\rangle_i\langle e| - |g\rangle_i\langle g|$. Here (e, g) refers to the excited and ground state of a two-level

atom, respectively and a labels the annihilation operator for a cavity photon. The Heisenberg-Langevin equations for these variables are:

$$\partial_t a(t) = -\left[\kappa + i\left(\omega_0 + \frac{U}{2N}\sum_{\ell=1}^{N}\sigma_\ell^z(t)\right)\right]a(t) - i\frac{g}{\sqrt{N}}\sum_{\ell=1}^{N}\left(\sigma_\ell^-(t) + \sigma_\ell^+(t)\right) + \sqrt{2\kappa}a_{\rm in}(t) \tag{12}$$

$$\partial_t \sigma_i^+(t) = i\left(\Delta + \frac{U}{N}a^\dagger(t)a(t)\right)\sigma_i^+(t) - i\frac{g}{\sqrt{N}}\sigma_i^z(t)\left(a(t) + a^\dagger(t)\right) - \frac{\gamma}{2}\sigma^+(t) + \mathcal{F}_i^+(t) \tag{13}$$

$$\partial_t \sigma_i^z(t) = 2\frac{g}{\sqrt{N}}\left((a(t) + a^\dagger(t)\right)\left(\sigma_i^-(t) - \sigma_i^+(t)\right)i - (1 + \sigma_i^z(t))\gamma + \mathcal{F}_i^z(t) \tag{14}$$

Here, $(a_{\rm in}(t), \mathcal{F}^z(t), \mathcal{F}^+(t), \mathcal{F}^-(t))$ are the usual fluctuating quantum mechanical noise operators with zero mean. They result from integrating out the bath of electromagnetic modes outside the cavity.

The reservoir correlation functions within the Markov approximation (that is, δ-correlated in time) are

$$\langle \mathcal{F}_i^z(t)\mathcal{F}_i^z(t')\rangle = 4\gamma\left(\bar{n}_\Delta\langle\sigma_i^-(t)\sigma_i^+(t')\rangle + (1 + \bar{n}_\Delta)\langle\sigma_i^+(t)\sigma_i^-(t')\rangle\right)\delta(t - t'), \tag{15}$$

$$\langle \mathcal{F}_i^+(t)\mathcal{F}_i^-(t')\rangle = \gamma\bar{n}_\Delta\delta(t - t')\langle\sigma_i^z(t)\sigma_i^z(t')\rangle, \tag{16}$$

$$\langle \mathcal{F}_i^-(t)\mathcal{F}_i^+(t')\rangle = \gamma(1 + \bar{n}_\Delta)\delta(t - t')\langle\sigma_i^z(t)\sigma_i^z(t')\rangle, \tag{17}$$

$$\langle a_{\rm in}^\dagger(t)a_{\rm in}(t')\rangle = \bar{n}_{\omega_0}\delta(t - t'), \tag{18}$$

$$\langle a_{\rm in}(t)a_{\rm in}^\dagger(t')\rangle = \delta(t - t')(1 + \bar{n}_{\omega_0}). \tag{19}$$

The single-particle occupation of the bath modes at the system frequencies ω_0 and Δ at temperature T is denoted by $\bar{n}_{\omega_0}$ and $\bar{n}_\Delta$, respectively. We can take the bath to be at zero temperature and set $\bar{n}_\Delta = \bar{n}_{\omega_0} = 0$ in what follows. In the remainder of the paper, we provide an analysis of these set of equations and try to connect our theoretical results to the recent experiment [11].

III. RESULTS

In this section, we first compute an analytic formula for the critical coupling for the onset of Dicke superradiance in the presence of atomic spontaneous emission. We then use this formula to determine an effective atomic loss rate for the experiment in Ref. [11]. As we argued earlier the formula is in fact the *exact solution* of the problem, even when the atomic loss is uncorrelated between individual sites. We close by searching for signatures of the additional loss channel γ in the cavity output spectrum and by computing the effective temperature of the system.

A. Critical coupling for onset of superradiance $g_c(\kappa, \gamma)$

We first transform Eqs. (12-14) into frequency space by the following relation:

$$O(t) = \frac{1}{2\pi}\int_{-\infty}^{\infty} e^{-i\nu t} O(\nu) d\nu, \quad O^\dagger(t) = \frac{1}{2\pi}\int_{-\infty}^{\infty} e^{-i\nu t} O^\dagger(-\nu) d\nu \,, \tag{20}$$

where the operator $O(t)$ is either of $\left(a(t), \sigma_i^+(t), \sigma_i^z(t), a_{\rm in}(t), \mathcal{F}_i^+(t), \mathcal{F}_i^z(t)\right)$ and $O^\dagger(t)$refers to either of $\left(a^\dagger(t), \sigma_i^-(t), a_{\rm in}^\dagger(t)\right)$. We then specifically make a distinction between the semi-classical steady states and the amplitude fluctuations around these values by linearising Eqs. (12-14). We define the fluctuation operators in frequency space by the relation

$$\sigma^+(\nu) = 2\pi \langle\sigma^+\rangle \delta(\nu) + \delta\sigma^+(\nu), \tag{21}$$

$$\sigma^z(\nu) = 2\pi \langle\sigma^z\rangle \delta(\nu) + \delta\sigma^z(\nu), \tag{22}$$

$$a(\nu) = 2\pi \sqrt{N} \langle a\rangle \delta(\nu) + \delta a(\nu) \,. \tag{23}$$

Where the set of steady-states $\langle\sigma^+\rangle$ and $\langle\sigma^z\rangle$ and $\langle a\rangle$ is given by equation Eqs. (30-33). Here, $\delta\sigma^+(\nu), \delta\sigma^z(\nu)$ and $\delta a(\nu)$ describe quantum fluctuations about the semi-classical steady-state and $\delta(\nu)$ denotes a delta function in frequency space. The equations for the amplitude fluctuations are generated by inserting Eqs. (21-23) into the Fourier transformed set of Eqs. (12-14). At long times, we may neglect second-order terms in the fluctuations by assuming that the steady-state values are large compared to the associated fluctuations in the thermodynamic limit $N \to \infty$. The linearized equations can be cast in matrix form

$$\boldsymbol{\mathcal{F}}(\nu) = \delta(\nu) f(\boldsymbol{\sigma}) + \boldsymbol{G}_R^{-1}(\nu) \cdot \boldsymbol{\delta\sigma}(\nu), \tag{24}$$

where the fluctuation (noise) operators are collected in the vectors $\delta\boldsymbol{\sigma}(\nu)$ ($\boldsymbol{\mathcal{F}}(\nu)$):

$$\delta\boldsymbol{\sigma}^T(\nu) = \left(\delta a(\nu), \delta a^\dagger(-\nu), \delta\sigma^+(\nu), \delta\sigma^-(-\nu), \delta\sigma^z(\nu)\right), \tag{25}$$

$$\boldsymbol{\mathcal{F}}^T(\nu) = \left(\sqrt{2\kappa} a_{\rm in}(\nu),\ \sqrt{2\kappa} a_{\rm in}^\dagger(-\nu), \mathcal{F}^+(\nu), \mathcal{F}^-(-\nu), \mathcal{F}^z(\nu)\right). \tag{26}$$

The inverse response function (retarded Green's function) $\boldsymbol{G_R^{-1}}(\nu)$ takes the form

$$\begin{pmatrix}
\frac{1}{2}iU\langle\sigma^z\rangle + \kappa - i\nu + i\omega_0 & 0 & ig & ig & i\frac{U}{2}\langle a\rangle \\
0 & -\frac{1}{2}iU\langle\sigma^z\rangle + \kappa - i\nu - i\omega_0 & -ig & -ig & -i\frac{U}{2}\langle a^\dagger\rangle \\
ig\langle\sigma^z\rangle - iU\langle a^\dagger\rangle\langle\sigma^+\rangle & ig\langle\sigma^z\rangle - iU\langle a\rangle\langle\sigma^+\rangle & -iU\langle a\rangle\langle a^\dagger\rangle + \frac{\gamma}{2} - i\Delta - i\nu & 0 & ig(\langle a\rangle + \langle a\rangle^\dagger) \\
iU\langle a^\dagger\rangle\langle\sigma^-\rangle - ig\langle\sigma^z\rangle & -ig\langle\sigma^z\rangle + iU\langle a\rangle\langle\sigma^-\rangle & 0 & iU\langle a\rangle\langle a^\dagger\rangle + \frac{\gamma}{2} + i\Delta - i\nu & -ig(\langle a\rangle + \langle a\rangle^\dagger) \\
2ig(\langle\sigma^+\rangle - \langle\sigma^-\rangle) & 2ig(\langle\sigma^+\rangle - \langle\sigma^-\rangle) & 2ig(\langle a\rangle + \langle a\rangle^\dagger) & -2ig(\langle a\rangle + \langle a\rangle^\dagger) & \gamma - i\nu
\end{pmatrix} \tag{27}$$

The notation indicates that the responses of the system $\boldsymbol{\delta\sigma}(\nu)$ to the "driving force" $\boldsymbol{\mathcal{F}}(\nu)$ is indeed described by the function $\boldsymbol{G}_R(\nu)$. The steady state contribution is encoded in $f(\boldsymbol{\sigma})$. We approach the phase transition from the normal phase, for which $\langle a\rangle = \langle\sigma^+\rangle = 0$ and assume the atoms to be fully polarized $\langle\sigma^z\rangle = -1$. Evaluating the condition for superradiance, $\lim_{\nu\to 0} \det[\boldsymbol{G}_{\boldsymbol{R}}^{-1}(\nu)] = 0$, yields the critical coupling

$$g_c(\gamma,\kappa,U) = \frac{\sqrt{\frac{\gamma^2}{4}+\Delta^2}\sqrt{\kappa^2+\left(\omega_0-\frac{U}{2}\right)^2}}{2\sqrt{\Delta\left(\omega_0-\frac{U}{2}\right)}}. \tag{28}$$

This formula recovers the known expression [10] in the limit $(U,\gamma)\to 0$ and the critical coupling known from [23] in the limit $\gamma\to 0$. It can be seen that the spontaneous emission γ "shifts" the atomic energy scale Δ and the photon loss rate κ shifts the cavity-frequency ω_0. As expected, the addition of spontaneous atomic emission leads to an increased value for the critical coupling g_c.

Comparing this value Eq. (28) for the critical coupling to Eq. (103) in Ref. 21, we note the structural similarity. However, the prefactor is different and this is due to the different nature of atomic decay processes included. Here, we included the conventional directed spontaneous emission into the spin-down state, while Ref. 21 included a dissipative dephasing term.

B. Comparison with Singapore experiment

In the Baden *et al.* experiment, the Dicke model was realized using cavity-assisted Raman transitions [11]. A sudden increase in the number of detected cavity photons upon ramping up the drive strength of an external laser has been associated with the threshold for Dicke superradiance. Some elements of the experiment we have already mentioned above in Subsec. II D.

Baden *et al.* [11] compared the experimentally observed threshold couplings to the conventional theory value without spontaneous emission [10, 23] and found a discrepancy: higher pump strengths than predicted were necessary to observe an increase in photon numbers.

In Fig. 1, we show that the experimental data for the critical coupling can be determined with our formula Eq. (28) and also places a range of the estimated values on the *effective* atomic decay rates γ_{eff}. We plot Eq. (28) against the dispersive shift ω_d. We make use of the relation $g_c^2(\kappa,\gamma)\propto P$, where P is the laser Power and $\Omega_r \propto \sqrt{P}$ is the Rabi frequency of the pump-laser. There is an overall proportionality constant, which is set by a comparison to the experimental values.

To make the mapping quantitative, we used the parameters given in Table I and further matched

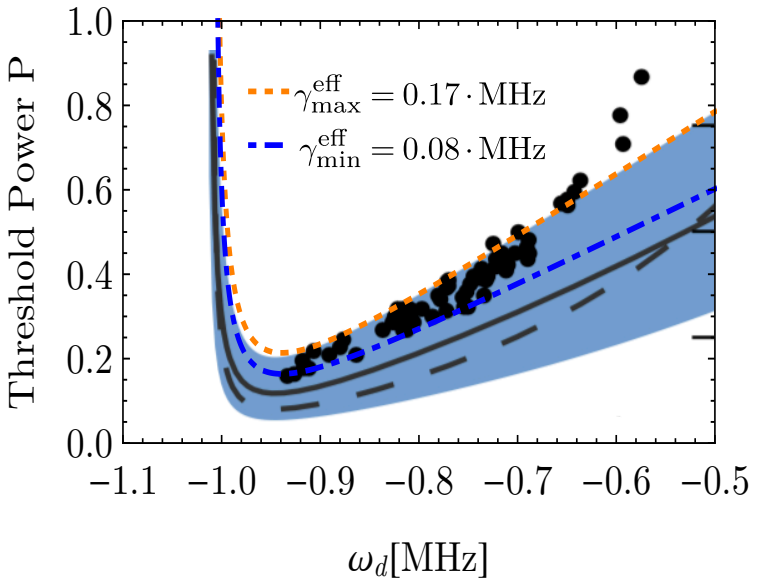


Figure 1. Threshold power P (normalized) for the onset of superradiance overlaying the experimental results [11] (Copyright (2014) by the American Physical Society) with the theoretical prediction according to Eq. (28) including an estimated effective spontaneous emission rate γ^{eff}. Here, γ^{eff} is not the fundamental single-atom spontaneous emission γ_{exc} of the transition directly coupling to the cavity. γ_{exc} is known and given in Table I. Rather, γ^{eff} should be regarded as an effective spin decay rate after eliminating the far-detuned excited state, possibly other decay channels, and other experimental imperfections. Gray, solid line: Theory curve for $\gamma \to 0$ limit of Eq. (28), taken from 11. Gray, dashed line: Theory curve taken from Ref. 11 without a differential Stark shift.

conventions:

$$\frac{U}{N} \to \frac{\delta}{N_\lambda}, \quad \omega_0 \to \omega_d - \eta, \quad \frac{g}{\sqrt{N}} \to \frac{\lambda}{\sqrt{N_\lambda}}, \quad \Delta \to \omega_0 \tag{29}$$

and $\delta = \frac{1}{3}\omega_d\left(\frac{\lambda_s}{\lambda_r} - 1\right)$ with $\frac{\lambda_s - \lambda_r}{\lambda_s + \lambda_r} \approx 0.028$ and the coupling is set as $\lambda \approx \lambda_r \approx \lambda_s$. Here, ω_d is the dispersive shift of the cavity resonance caused by the presence of atoms in the lower hyperfine state $|g\rangle$ and $N_\lambda \approx N/3$ is the number of atoms in the coupled states $|e\rangle$ and $|g\rangle$. (λ_r, λ_s) refers to the effective coupling strength of the co- and counter rotating terms in the Dicke model to the hyperfine-split levels $|e\rangle, |g\rangle$ as realized by the two Raman coupling beams.

One possible way to estimate the inherited decay rate of the spin-up state from the fundamental decay of the excited state is $\gamma_{\text{eff}} = \frac{1}{4}\left(\frac{\gamma_{\text{exc}}}{2\pi}\right)\left(\frac{\Omega_r}{\Delta_r}\right)^2 \propto P$, which is proportional to the population in the excited state. But other experimental imperfections need to be accounted for to make this quantitative. Such non-linear effects might also be at the root of the upturn in the experimental

$\omega_0 + \zeta$	η	ζ	λ_s/λ_r	κ	$\gamma_{\rm exc}$
$-2\pi \times 12.02\,$MHz	$-2\pi \times 1\,$MHz	$-2\pi \times 12.15\,$MHz	1.058	$-2\pi \times 0.07\,$MHz	$2\pi \times 3.0\;$ MHz

Table I. Set of experimental values from [11] used for the comparison of theory and experiment in Fig. 1. We also give the fundamental atomic decay rate of the excited state level coupling to the cavity $\gamma_{\rm exc}$.

data for the critical coupling strength at larger values of ω_d in Fig. 1.

An additional interesting regime to pin down the effects of γ is the critical region for small longitudinal spin detuning Δ. From the critical coupling Eq. (28), we observe that $g_c(\gamma, \kappa)$ becomes large for small Δ provided γ is finite. By contrast in the strict $\gamma \to 0$ limit $g_c(\gamma = 0, \kappa)$ *decreases* for small Δ. New rounds of data-taking can access this and other regimes with improved accuracy [24].

C. Non-equilibrium steady states for spins and photons

In this section, we discuss the steady-state operator expectation values $\langle a \rangle, \langle \sigma^+ \rangle, \langle \sigma^z \rangle$, where $\langle a \rangle$ is the complex field amplitude that accounts for a coherent photon condensate, $\langle \sigma^+ \rangle$ is the complex atomic polarization amplitude and $\langle \sigma^z \rangle$ measures the atomic population imbalance. The dynamics of the expectation values is given by Eqs. (12-14), where all operators are replaced by their average value ($\sqrt{N}\langle a \rangle, \langle \sigma^+ \rangle, \langle \sigma^z \rangle$). In the semi-classical picture for a spin-1/2 system we construct the expectation value of the spin-vector $\langle \boldsymbol{S}(t) \rangle = (\langle \sigma^x(t) \rangle, \langle \sigma^y(t) \rangle, \langle \sigma^z(t) \rangle)^T$. It defines the orientation of the averaged atomic Bloch vector. The non-equilibrium Bloch dynamics of the collective angular momentum without spontaneous emission was studied in Ref. 23.

An analytical solution for the semiclassical steady-states ($\partial_t \langle \sigma^\alpha(t) \rangle) = 0$ and $\partial_t \langle a(t) \rangle = 0$ is accessible for the $U = 0$ case. We solve the system of non-linear equations for the fixed points to obtain the steady-states. For $g < g_c$ the only steady-state is $\langle a \rangle = \langle \sigma^+ \rangle = 0$ and $\langle \sigma^z \rangle = -1$. This is the empty atom-cavity system as the spontaneous atomic decay and photon loss depletes the system of all excitations. The mean-field expectation values for the fields in the superradiant

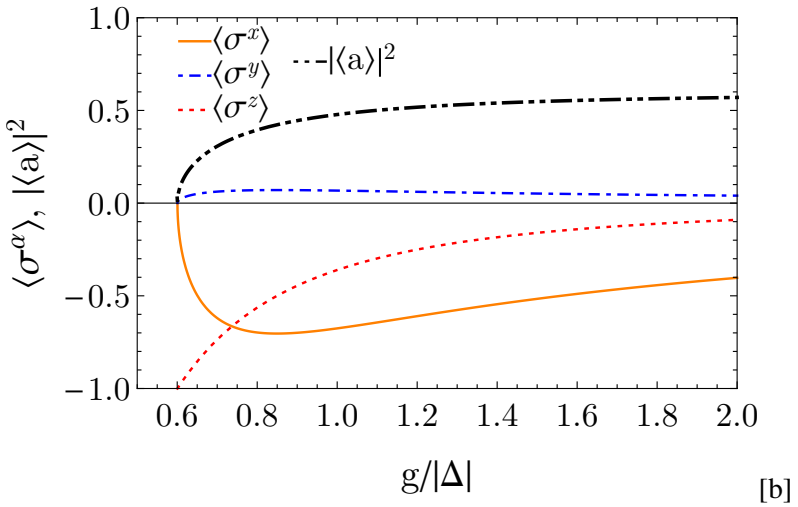


Figure 2. Stable steady-state field amplitudes $|\langle a\rangle|^2$ and $(\langle\sigma^x\rangle, \langle\sigma^y\rangle, \langle\sigma^z\rangle)$ in the superradiant phase $g > g_c$ for the set of parameters $\gamma = \kappa = 0.2|\Delta|, \omega_0 = 1.4|\Delta|$, where $g_c/\Delta \approx 0.6$

phase $g > g_c$ are:

$$\langle a\rangle = \frac{\sqrt{\frac{\kappa^2+\omega_0^2}{\omega_0}}\sqrt{\Delta\left(1-\frac{J_c}{J}\right)}}{\sqrt{2}(-\omega_0+i\kappa)}, \tag{30}$$

$$\langle\sigma^x\rangle = \frac{1}{2}\left(\langle\sigma^+\rangle + i\langle\sigma^-\rangle\right) = \pm\frac{\sqrt{\Delta(J-J_c)}}{\sqrt{2}J}, \tag{31}$$

$$\langle\sigma^y\rangle = \frac{1}{2}\left(\langle\sigma^+\rangle - i\langle\sigma^-\rangle\right) = \mp\gamma\frac{\sqrt{\Delta(J-J_c)}}{2\sqrt{2}\Delta J}, \tag{32}$$

$$\langle\sigma^z\rangle = -(J_c/J). \tag{33}$$

Here the different signs for the steady-state solutions reflect the $\mathbb{Z}_2$ symmetry, see Eq. (5), and we have abbreviated the notation by defining

$$J = \frac{g^2\omega_0}{\kappa^2+\omega_0^2}, \tag{34}$$

$$J_c = \frac{\gamma^2+4\Delta^2}{16\Delta}. \tag{35}$$

A plot of Eqs. (30-33) is given in Fig. 2. The critical coupling strength g_c for the superradiant phase transition (28) can also be obtained by equating Eqs. (34) and (35). For $\Delta < 0$ there is no real-valued solution for the magnetizations $(\langle\sigma^x\rangle, \langle\sigma^y\rangle)$ which means that this regime excludes a stable photon condensate.

Note that the solutions for the mean-field expectation values do not recover the solutions that

are obtained by taking the $\gamma \to 0$ limit from the outset in Eqs. (12-14). This is because the steady-state is usually approached with a rate $\propto 1/\gamma$ which diverges in the $\gamma \to 0$ limit.

D. Cavity output spectrum

The internal dynamics of the atom-cavity system can be probed by analyzing the light that leaks from the cavity mirrors. We employ standard input-output theory for the quantum Langevin equations [10, 25, 26] to calculate the cavity spectrum. The input-fields are related to the output fields by the relation

$$a_{\text{out}}(\nu) = \sqrt{2\kappa}a(\nu) - a_{\text{in}}(\nu), \tag{36}$$

$$a^{\dagger}_{\text{out}}(-\nu) = \sqrt{2\kappa}a^{\dagger}(-\nu) - a^{\dagger}_{\text{in}}(-\nu). \tag{37}$$

The annihilation operators $(a_{\text{out}}(\nu), a_{\text{in}}(\nu), a(\nu))$ correspond to the output field, the input field, and the intra cavity field, respectively. For a vacuum field input, the correlations of the noise operators (see Eqs. (15-19))in frequency space are

$$\langle a_{\text{in}}(\nu')a^{\dagger}_{\text{in}}(-\nu)\rangle = \delta(\nu+\nu'), \tag{38}$$

$$\langle \mathcal{F}^{-}(-\nu')\mathcal{F}^{+}(\nu)\rangle = \gamma\delta(\nu+\nu'), \tag{39}$$

$$\langle \mathcal{F}^{z}(\nu)\mathcal{F}^{z}(\nu')\rangle = 2\gamma(1+\langle\sigma^{z}\rangle)\delta(\nu+\nu'). \tag{40}$$

We solve Eq. (24) for the fluctuations around the photon condensate and omit the coherent contribution coming from the zero-frequency components specified by $f(\boldsymbol{\sigma})$. Making use of Eqs. (36-38), the cavity fluorescence spectrum $S(\nu)$ (for a vacuum input field) accounting for the fluctuations around the steady state is

$$S(\nu) = \langle a^{\dagger}_{\text{out}}(\nu)a_{\text{out}}(\nu)\rangle = 2\kappa\,\langle\delta a^{\dagger}(\nu)\delta a(\nu)\rangle = 2\kappa\int_{-\infty}^{\infty} e^{-i\nu\tau}\,\langle\delta a^{\dagger}(0)\delta a(\tau)\rangle\,d\tau. \tag{41}$$

By employing Eqs. (15-19) the cavity spectrum in the $g < g_c$ case for the steady-states $\langle\sigma^{+}\rangle = \langle\sigma^{-}\rangle = 0$ and $\langle\sigma^{z}\rangle = -1$ becomes

$$S(\nu) = \frac{8g^2\kappa\left(\gamma\left(\gamma^2+4(\Delta-\nu)^2\right)\left(\kappa^2+(\nu+\omega_0^2\right)+32\Delta^2g^2\kappa\right)}{|\Omega(\nu)|^2}, \tag{42}$$

$$\Omega(\nu) = (\kappa-i\nu)^2\left(4\Delta^2+(\gamma-2i\nu)^2\right)+\omega_0^2\left(4\Delta^2+(\gamma-2i\nu)^2\right)-16\Delta g^2\omega_0. \tag{43}$$

The poles in (42) correspond to the hybridized atom-cavity eigenmodes of the system. They are given by the solutions to the equation $\det[\boldsymbol{G}_{\boldsymbol{R}}^{-1}(\nu)] = 0$ where $\boldsymbol{G}_{\boldsymbol{R}}^{-1}(\nu)$ is defined in Eq. (27). Close to

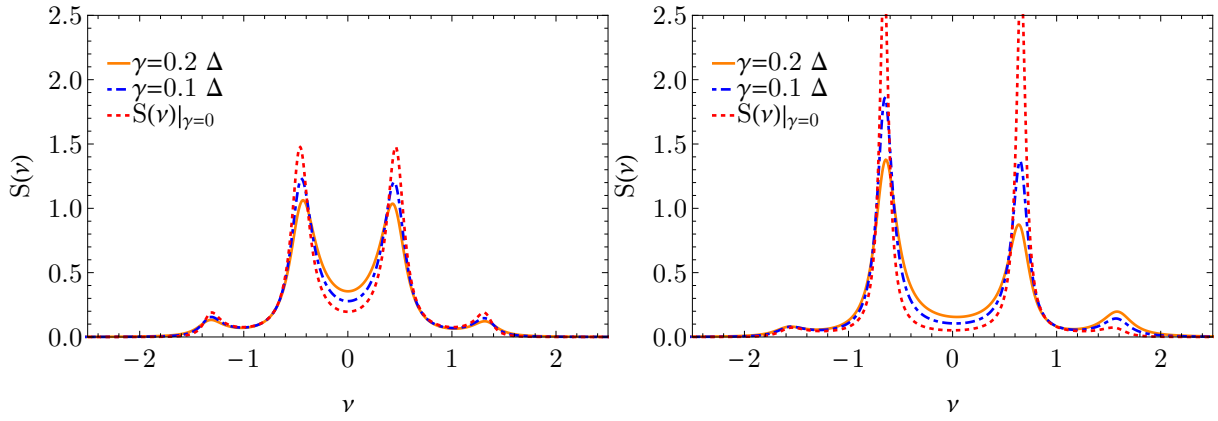


Figure 3. Cavity spectra in the vacuum phase with spontaneous emission and a broken frequency symmetry $S(\nu) \neq S(-\nu)$. We have normalized the spectra such that $\int S(\nu)d\nu = 1$. When there is no atomic spontaneous emission ($S(\nu)|_{\gamma=0}$), the frequency symmetry of the cavity spectrum is restored. Parameters: $\kappa = 0.2|\Delta|, g = 0.4|\Delta| < g_c$. The figure (a) shows the on-resonance spectrum:$\omega_0 = 1.0|\Delta|$, the figure (b) shows the off-resonance spectrum at $\omega_0 = 1.4|\Delta|$

.

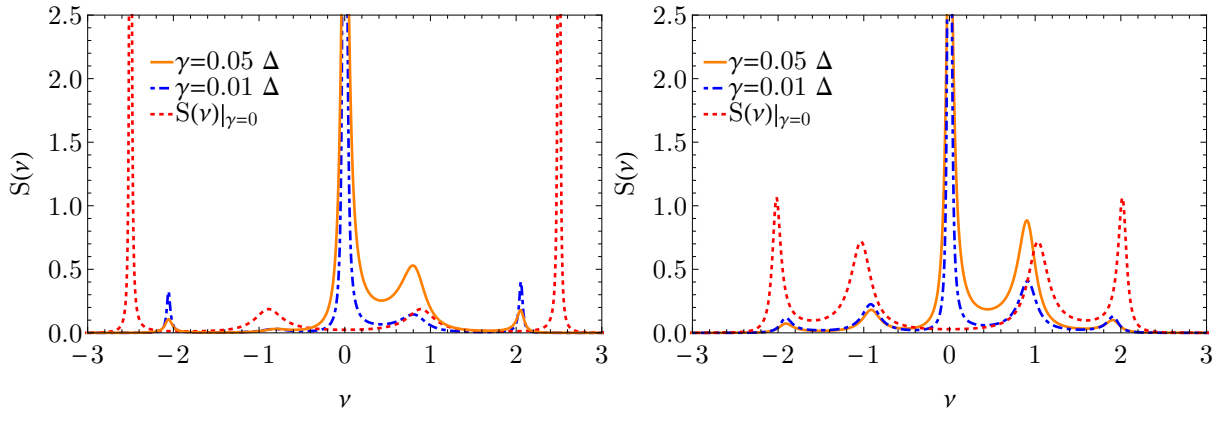


Figure 4. Cavity spectra in the superradiant regime with spontaneous emission and a broken frequency symmetry $S(\nu) \neq S(-\nu)$. We have normalized the spectra such that $\int S(\nu)d\nu = 1$. Parameters: $\kappa = 0.2|\Delta|, \gamma = 0.1|\Delta|, g = 0.8|\Delta| > g_c$. Here, $S(\nu)|_{\gamma=0}$ is understood as solving the Eqs. (12)-(14) on a mean-field level by setting $\gamma = 0$ from the outset and calculating $S(\nu)$ with Eq. (41), see [10]. In figure (a) the system is on resonance: $\omega_0 = |\Delta|$, in figure (b) it is off resonance: $\omega_0 = 1.4|\Delta|$.

the superradiance transition, two poles become purely imaginary and characterize the overdamped dynamics at the phase transition, see e.g. [21]. At the transition a single critical mode approaches the origin linearly in $(g - g_c)$. The corresponding equations for $\gamma \neq 0$ can be found in the appendix, Eqs. (A10-A13).

The output spectrum in the presence of spontaneous atomic decay is no longer symmetric under inversion on the frequency axis $S(\nu) \neq S(-\nu)$, see Fig. 3. This is due to the fact that in the presence of atomic decay, cavity photons can exit the cavity in two different ways. Either directly via the cavity decay channel $\sim \kappa$ or indirectly via exciting an atom and subsequently decaying via spontaneous emission $\sim \gamma$. The latter process of combined excitation and decay prefers photon states with positive frequency. This leads to a reduction of $S(\nu)$ for positive frequencies and introduces the mentioned asymmetry in the photon output spectrum. In the limit of vanishing spontaneous emission, the cavity spectrum collapses to the familiar result [10] and the frequency symmetry is restored:

$$\lim_{\gamma \to 0} S(\nu) = \frac{16\Delta^2 g^4 \kappa^2}{|\Omega'(\nu)|^2}, \tag{44}$$

$$\Omega'(\nu) = (\Delta - \nu)(\Delta + \nu)(\kappa - i\nu)^2 + \omega_0^2(\Delta - \nu)(\Delta + \nu) - 4\Delta g^2 \omega_0. \tag{45}$$

A typical cavity output spectrum for the superradiant case $g > g_c$ is defined in Eq. (A7) and can be seen in Fig. 4. Here $\gamma > 0$ leads to a broadening of the spectrum and a pronounced weight of $S(\nu)$ at positive frequencies $\nu > 0$ due to the dominant effect of stimulated emission and absorption over spontaneous decay effects. In Fig. 4 and Fig. 3 the expression $S(\nu)|_{\gamma=0}$ refers to the cavity spectrum that is obtained by setting $\gamma = 0$ in Eqs. (12)-(14) and by then following the same procedure as outlined above, see [10].

E. Effective temperature

In Ref. 21, the authors outlined an approach to extract the effective temperature of open quantum-optical systems. The idea is to map the photon equation of motion to classical Langevin equations and read off the effective temperatures as a function of the noise correlation functions. Here, we generalize this analysis to include atomic spontaneous emission γ and extract the corresponding effective temperature. To that end, we define the real part of the photon component $\delta x(\nu)$

and the corresponding noise operator $\mathcal{F}_x(\nu)$:

$$\delta x(\nu) = \frac{1}{\sqrt{2\omega_0}}\left(\delta a(\nu) + \delta a^\dagger(-\nu)\right), \tag{46}$$
$$\mathcal{F}_x(\nu) = \frac{1}{\sqrt{2\omega_0}}\left[\mathcal{F}_a(\nu)r(\nu) + \mathcal{F}_{a^\dagger}(-\nu)r^*(-\nu) + \mathcal{F}^+(\nu)p(\nu) + \mathcal{F}^-(-\nu)p^*(-\nu)\right].$$

Here, $\mathcal{F}_a \equiv \sqrt{2\kappa}a_{\text{in}}$ and the fluctuation operators $\delta a(\nu), \delta a^\dagger(-\nu)$ are defined in terms of noise operators in Eqs. (A1), (A2). We evaluate them at the critical point, which is approached from the normal phase ($\langle a\rangle = \langle\sigma^+\rangle = 0$, $\langle\sigma^z\rangle = -1$). The complex functions $r(\nu)$ and $p(\nu)$ are defined as

$$r(\nu) = (\kappa - i(\nu + \omega_0)), \tag{47}$$
$$p(\nu) = -\frac{4g(\gamma - 2i(\Delta + \nu))}{3\Delta^2 + (\gamma - 2i\nu)}\omega_0. \tag{48}$$

In the δx-channel, the response of the fluctuations to the "driving force" $\mathcal{F}_x(\nu)$ is

$$\mathcal{F}_x(\nu) = \left(\omega_0^2 - \frac{16\Delta g^2}{4\Delta^2 + (\gamma - 2i\nu)^2}\omega_0 + (\kappa - i\nu)^2\right)\delta x(\nu). \tag{49}$$

At low frequencies, equation Eq. (49) resembles a Langevin equation for a classical particle subject to a harmonic potential with oscillation frequency

$$\alpha^2 = \left(\omega_0^2 - \frac{16\Delta g^2}{\gamma^2 + 4\Delta^2}\omega_0 + \kappa^2\right) \tag{50}$$

and an effective damping constant

$$\tilde{\kappa} = 2\left(\kappa + \frac{32\gamma\Delta g^2\omega_0}{\left(\gamma^2 + 4\Delta^2\right)^2}\right). \tag{51}$$

This illustrates the fact that the photon can decay via two channels: directly via κ and by first converting it to an atomic excitation, which can then decay via γ.

We may now identify the effective temperature of the system at the critical point as

$$2\tilde{\kappa}T_{\text{eff}}^{\text{crit}} = \lim_{\nu\to 0}\frac{1}{2}\left\langle\mathcal{F}_x(\nu)\mathcal{F}_x(-\nu) + \mathcal{F}_x(-\nu)\mathcal{F}_x(\nu)\right\rangle\Big|_{g=g_c}, \tag{52}$$
$$T_{\text{eff}}^{\text{crit}} = \frac{\left(\gamma^2 + 4\Delta^2\right)\left(\kappa^2 + \omega_0^2\right)(\gamma\omega_0 + 2\Delta\kappa)}{8\Delta\omega_0\left(\gamma^2\kappa + 2\gamma\left(\kappa^2 + \omega_0^2\right) + 4\Delta^2\kappa\right)}. \tag{53}$$

In the presence of only a single decay channel, we recover the known cases [21]

$$\lim_{\gamma\to 0} T_{\text{eff}}^{\text{crit}} = \frac{\kappa^2 + \omega_0^2}{4\omega_0}, \tag{54}$$
$$\lim_{\kappa\to 0} T_{\text{eff}}^{\text{crit}} = \frac{\frac{\gamma^2}{4} + \Delta^2}{4\Delta}. \tag{55}$$

For certain parameter regimes $(\omega_0, \Delta, k, \gamma)>0$ the effective temperature in the presence of spontaneous decay $\gamma > 0$ can be smaller than in the absence of atomic decay $\gamma = 0$, i.e. $T_{\text{eff}}^{\text{crit}} < \lim_{\gamma\to 0} T_{\text{eff}}^{\text{crit}}$.

This happens for $0 < \Delta < \frac{\kappa^2+\omega_0^2}{\omega_0}$ and $0 < \gamma < 2\sqrt{\frac{\Delta\left(\omega_0(\omega_0-\Delta)+\kappa^2\right)}{\omega_0}}$, i.e. for system parameters for which spontaneous atomic decay is energetically favorable over cavity photon loss.

IV. CONCLUSIONS

In this paper we investigated the effect of atomic spontaneous emission on the non-equilibrium steady-states of the open Dicke model. We argued that a site decoupling mean-field ansatz gives access to the exact solution of the problem in the thermodynamic limit. By determining the critical coupling $g_c(\kappa, \gamma)$ for the onset of superradiance as an explicit function of the spontaneous emission rate γ, we were able to compare this result to experimental values for the onset of superradiance as measured by Baden *et al.* [11]. Thereby we estimated an upper and lower bound for an effective spontaneous emission rate that might explain the experimentally observed discrepancy between previous analytical calculations and experimental measurements. Moreover, we have quantified the sideband asymmetry in the cavity-output spectrum due to atomic spontaneous emission.

An interesting future direction is the inclusion of additional short-range interactions between the atoms, for example by weakly dressing the spin-up level with a Rydberg state [27]. This interaction will now compete with cavity-mediated, long-range interactions and the various drive and decay processes. Moreover, changing the lattice geometry and using space-dependent pump fields could enable synthesis of exotic, open quantum magnets whose properties are shaped by quantum fluctuations of the light field.

ACKNOWLEDGMENTS

We thank M. Barrett for insightful explanations of experimental data. We also thank S. Diehl and A. Rosch for helpful discussions. This work was supported by the Leibniz Prize of A. Rosch and by the German Research Foundation (DFG) through the Institutional Strategy of the University of Cologne within the German Excellence Initiative (ZUK 81).

Appendix A: Details of calculation for cavity spectrum

We detail the calculations performed in Sec.III D to obtain the cavity spectrum $S(\nu)$ that is defined in Eq. (41). The fluctuations $\delta a(\nu), \delta a^\dagger(\nu)$ around the photon condensate are given as

$$\delta a(\nu) = a_{\rm in}^\dagger(-\nu) f(\nu) + a_{\rm in}(\nu) g(\nu) + \mathcal{F}_-(-\nu) m(\nu) + \mathcal{F}_+(\nu) h(\nu) + \mathcal{F}^z(\nu)\ell(\nu) \tag{A1}$$

$$\delta a^\dagger(-\nu) = a^+(-\nu)_{\rm in} g^\dagger(-\nu) + a_{\rm in}(\nu) f^\dagger(-\nu) + \mathcal{F}^-(-\nu) h^\dagger(-\nu) + \mathcal{F}^\dagger(\nu) m^\dagger(-\nu) + \mathcal{F}_z(\nu)\ell^\dagger(-\nu) \tag{A2}$$

Where the functions $\ell(\nu), h(\nu), f(\nu)$ are

$$\begin{aligned} D(\nu) =& -i(\gamma - i\nu)\left(4\Delta^2 + (\gamma - 2i\nu)^2\right)\left(\omega_0^2 + (\kappa - i\nu)^2\right) + 32\Delta g^3\omega_0(\langle a^\dagger\rangle + \langle a\rangle)(\langle\sigma^-\rangle - \langle\sigma^+\rangle) \\ & - 8ig^2\left((\langle a^\dagger\rangle + \langle a\rangle)^2(\gamma - 2i\nu)(\kappa - i\nu)^2 + \omega_0^2(\langle a^\dagger\rangle + \langle a\rangle)^2(\gamma - 2i\nu) + 2\Delta\omega_0\langle\sigma^z\rangle(\gamma - i\nu)\right) \\ D(\nu)f(\nu) =& -16i\Delta g^2\kappa\left(2g(\langle a^\dagger\rangle + \langle a\rangle)(\langle\sigma^-\rangle - \langle\sigma^+\rangle) + \langle\sigma^z\rangle(-\nu - i\gamma)\right) \qquad \text{(A3)} \\ D(\nu)h(\nu) =& -2g\sqrt{2\kappa}(\kappa - i(\nu + \omega_0))\left(8g^2(\langle a^\dagger\rangle + \langle a\rangle)^2 + (\gamma - i\nu)(\gamma + 2i(\Delta - \nu))\right) \qquad \text{(A4)} \\ D(\nu)\ell(\nu) =& -8\Delta g^2\sqrt{2\kappa}(\langle a^\dagger\rangle + \langle a\rangle)(\kappa - i(\nu + \omega_0)) \qquad \text{(A5)} \end{aligned}$$

By employing Eqs. (15-19) we can identify the cavity-spectrum as

$$S(\nu) = \left(f^\dagger(\nu)f(\nu) + \gamma h^\dagger(\nu)h(\nu) + 2\gamma(1 + \langle\sigma^z\rangle)\ell(\nu)\ell^\dagger(\nu)\right) \tag{A6}$$

The cavity spectrum for the superradiant case for $g > g_c$ is given by

$$S(\nu) = \frac{s(\nu)}{\Omega(\nu)\Omega^\dagger(\nu)} \tag{A7}$$

$$\begin{aligned} \Omega(\nu) =& -i(\gamma - i\nu)\left(4\Delta^2 + (\gamma - 2i\nu)^2\right)\left(\omega_0^2 + (\kappa - i\nu)^2\right) + 32\Delta g^3\omega_0(\langle a^\dagger\rangle + \langle a\rangle)(\langle\sigma^-\rangle - \langle\sigma^+\rangle) \\ & - 8ig^2\left((\langle a^\dagger\rangle + \langle a\rangle)^2(\gamma - 2i\nu)(\kappa - i\nu)^2 + \omega_0^2(\langle a^\dagger\rangle + \langle a\rangle)^2(\gamma - 2i\nu) + 2\Delta\omega_0\langle\sigma^z\rangle(\gamma - i\nu)\right) \end{aligned} \tag{A8}$$

$$\begin{aligned} s(\nu) =& 8g^2\kappa\left(\gamma\left(\gamma^2 + \nu^2\right)\left(\gamma^2 + 4(\Delta - \nu)^2\right)\left(\kappa^2 + (\nu + \omega_0)^2\right)\right. \\ & + 64g^4(\langle a^\dagger\rangle + \langle a\rangle)^2\left(\gamma(\langle a^\dagger\rangle + \langle a\rangle)^2\left(\kappa^2 + (\nu + \omega_0)^2\right) - 2\Delta^2\kappa(\langle\sigma^-\rangle - \langle\sigma^+\rangle)^2\right) \\ & + 128i\gamma\Delta^2 g^3\kappa\langle\sigma^z\rangle(\langle a^\dagger\rangle + \langle a\rangle)(\langle\sigma^-\rangle - \langle\sigma^+\rangle) \\ & + 16g^2\left(\gamma(\langle a^\dagger\rangle + \langle a\rangle)^2\left(\gamma^2 + 2\left(\Delta^2 + \Delta\nu - \nu^2\right)\right)\left(\kappa^2 + (\nu + \omega_0)^2\right)\right. \\ & \left.\left. + 2\Delta^2\kappa\langle\sigma^z\rangle^2\left(\gamma^2 + \nu^2\right) + 2\gamma\Delta^2\langle\sigma^z\rangle(\langle a^\dagger\rangle + \langle a\rangle)^2\left(\kappa^2 + (\nu + \omega_0)^2\right)\right)\right) \end{aligned} \tag{A9}$$

At the phase transition, there are two poles that become purely imaginary and describe the over-damped dynamics. The corresponding expressions are obtained by expanding $\mathrm{Det}[\boldsymbol{G_R^{-1}}(\nu)] = 0$ up

to second-order in the frequency. We refer to the solutions of the resulting quadratic equation by (ν_1, ν_2). The first pole vanishes linearly in $(g - g_c)$ and is given as:

$$\nu_1 = \frac{8i\Delta\omega_0\left(\gamma^2 + 4\Delta^2\right)(g - g_c)(g + g_c)}{\kappa\left(\gamma^2 + 4\Delta^2\right)^2 + 32\gamma\Delta g_c^2\omega_0} \tag{A10}$$

The residual pole at $g = g_c$ is

$$\nu_2 = -\frac{2i\left(\gamma^2\kappa + 2\gamma\left(\kappa^2 + \omega_0^2\right) + 4\Delta^2\kappa\right)}{\gamma^2 + 8\gamma\kappa + 4\left(\Delta^2 + \kappa^2 + \omega_0^2\right)} \tag{A11}$$

$$\lim_{\gamma\to 0}\nu_2 = -i\kappa\frac{2\Delta^2}{\Delta^2 + \kappa^2 + \omega_0^2} \tag{A12}$$

$$\lim_{\kappa\to 0}\nu_2 = -i\gamma\frac{\omega_0^2}{\frac{\gamma^2}{4} + \left(\Delta^2 + \omega_0^2\right)} \tag{A13}$$

Appendix B: Details of calculation for effective temperature

We detail the calculation of the effective temperature in Sec. III E for the Dicke-phase transition in the presence of spontaneous atomic decay. The stochastic force operator satisfies the relation $\left[\mathcal{F}_x(-\nu)\right]^\dagger = \mathcal{F}_x(\nu)$ and obeys the commutation relation:

$$\frac{1}{2}\left\langle\mathcal{F}_x(\nu)\mathcal{F}_x(\nu') + \mathcal{F}_x(\nu')\mathcal{F}_x(\nu)\right\rangle = \delta(\nu + \nu')\left(\frac{2\kappa}{4\omega_0}\left[r(\nu)r^\dagger(-\nu') + r(\nu')r^\dagger(-\nu)\right] + \frac{\gamma}{4\omega_0}\left[p(\nu)p^\dagger(-\nu') + p(\nu')p^\dagger(-\nu)\right]\right) \tag{B1}$$

Where $p(\nu)$ and $r(\nu)$ are given by Eq. (47) and by Eq. (48). At low frequencies the right-hand side of Eq. (49) evaluates to

$$\left(\omega_0^2 - \frac{16\Delta g^2}{\gamma^2 + 4\Delta^2}\omega_0 + \kappa^2\right) - 2i\nu\left(\kappa + \frac{32\gamma\Delta g^2\omega_0}{\left(\gamma^2 + 4\Delta^2\right)^2}\right) + O(\nu^2) \tag{B2}$$

and the commutation relation at $\nu' = -\nu$, see Eq. (B1), evaluates to:

$$\frac{1}{2}\left\langle\mathcal{F}_x(\nu)\mathcal{F}_x(\nu') + \mathcal{F}_x(\nu')\mathcal{F}_x(\nu)\right\rangle \approx \frac{\kappa}{\omega_0}\left(\kappa^2 + \omega_0^2\right) + \frac{\gamma}{4\omega_0}\frac{32g^2}{\gamma^2 + 4\Delta^2}\omega_0^2 + O(\nu^2) \tag{B3}$$

[1] C. Gardiner and P. Zoller, *The Quantum World of Ultra-Cold Atoms and Light Book II: The Physics of Quantum-Optical Devices*. World Scientific, first ed., 2015.

[2] J. Klinder, H. Keßler, M. R. Bakhtiari, M. Thorwart, and A. Hemmerich, "Observation of a superradiant mott insulator in the dicke-hubbard model," *Phys. Rev. Lett.*, vol. 115, p. 230403, Dec 2015.

[3] R. Landig, L. Hruby, N. Dogra, M. Landini, R. Mottl, T. Donner, and T. Esslinger, "Quantum phases from competing short- and long-range interactions in an optical lattice," *Nature*, vol. 532, pp. 476–479, 04 2016.

[4] A. Neuzner, M. Körber, O. Morin, S. Ritter, and G. Rempe, "Interference and dynamics of light from a distance-controlled atom pair in an optical cavity," *Nat Photon*, vol. 10, pp. 303–306, 05 2016.

[5] P. Strack and S. Sachdev, "Dicke quantum spin glass of atoms and photons," *Phys. Rev. Lett.*, vol. 107, p. 277202, Dec 2011.

[6] S. Gopalakrishnan, B. L. Lev, and P. M. Goldbart, "Frustration and glassiness in spin models with cavity-mediated interactions," *Phys. Rev. Lett.*, vol. 107, p. 277201, Dec 2011.

[7] M. Buchhold, P. Strack, S. Sachdev, and S. Diehl, "Dicke-model quantum spin and photon glass in optical cavities: Nonequilibrium theory and experimental signatures," *Phys. Rev. A*, vol. 87, p. 063622, Jun 2013.

[8] K. Hepp and E. H. Lieb, "On the superradiant phase transition for molecules in a quantized radiation field: the dicke maser model," *Annals of Physics*, vol. 76, no. 2, pp. 360 – 404, 1973.

[9] Y. K. Wang and F. T. Hioe, "Phase transition in the dicke model of superradiance," *Phys. Rev. A*, vol. 7, pp. 831–836, Mar 1973.

[10] F. Dimer, B. Estienne, A. S. Parkins, and H. J. Carmichael, "Proposed realization of the dicke-model quantum phase transition in an optical cavity qed system," *Phys. Rev. A*, vol. 75, p. 013804, Jan 2007.

[11] M. P. Baden, K. J. Arnold, A. L. Grimsmo, S. Parkins, and M. D. Barrett, "Realization of the dicke model using cavity-assisted raman transitions," *Phys. Rev. Lett.*, vol. 113, p. 020408, Jul 2014.

[12] A. T. Black, H. W. Chan, and V. Vuletić, "Observation of collective friction forces due to spatial self-organization of atoms: From rayleigh to bragg scattering," *Phys. Rev. Lett.*, vol. 91, p. 203001, Nov 2003.

[13] K. Baumann, C. Guerlin, F. Brennecke, and T. Esslinger, "Dicke quantum phase transition with a superfluid gas in an optical cavity," *Nature*, vol. 464, pp. 1301–1306, 2010.

[14] F. Brennecke, R. Mottl, K. Baumann, R. Landig, T. Donner, and T. Esslinger, "Real-time observation of fluctuations at the driven-dissipative dicke phase transition," vol. 110, no. 29, pp. 11763–11767, 2013.

[15] F. Piazza, P. Strack, and W. Zwerger, "Bose-einstein condensation versus dicke-hepp-lieb transition in an optical cavity," *Annals of Physics*, vol. 339, p. 135, 2013.

[16] M. Kulkarni, B. Öztop, and H. E. Türeci, "Cavity-mediated near-critical dissipative dynamics of a driven condensate," *Phys. Rev. Lett.*, vol. 111, p. 220408, Nov 2013.

[17] G. Kónya, G. Szirmai, and P. Domokos, "Damping of quasiparticles in a bose-einstein condensate coupled to an optical cavity," *Phys. Rev. A*, vol. 90, p. 013623, Jul 2014.

[18] F. Piazza and P. Strack, "Quantum kinetics of ultracold fermions coupled to an optical resonator," *Phys. Rev. A*, vol. 90, p. 043823, Oct 2014.

[19] J. D. Thompson, T. G. Tiecke, N. P. de Leon, J. Feist, A. V. Akimov, M. Gullans, A. S. Zibrov, V. Vuletić, and M. D. Lukin, "Coupling a single trapped atom to a nanoscale optical cavity," *Science*, vol. 340, no. 6137, pp. 1202–1205, 2013.

[20] D. E. Chang, J. I. Cirac, and H. J. Kimble, "Self-organization of atoms along a nanophotonic waveguide," *Phys. Rev. Lett.*, vol. 110, p. 113606, Mar 2013.

[21] E. G. D. Torre, S. Diehl, M. D. Lukin, S. Sachdev, and P. Strack, "Keldysh approach for nonequilibrium phase transitions in quantum optics: Beyond the dicke model in optical cavities," *Phys. Rev. A*, vol. 87, p. 023831, Feb 2013.

[22] H. Habibian, A. Winter, S. Paganelli, H. Rieger, and G. Morigi, "Bose-glass phases of ultracold atoms due to cavity backaction," *Phys. Rev. Lett.*, vol. 110, p. 075304, Feb 2013.

[23] M. J. Bhaseen, J. Mayoh, B. D. Simons, and J. Keeling, "Dynamics of nonequilibrium dicke models," *Phys. Rev. A*, vol. 85, p. 013817, Jan 2012.

[24] M. Barrett, Private Communication.

[25] M. J. Collett and C. W. Gardiner, "Squeezing of intracavity and traveling-wave light fields produced in parametric amplification," *Phys. Rev. A*, vol. 30, pp. 1386–1391, Sep 1984.

[26] C. W. Gardiner and M. J. Collett, "Input and output in damped quantum systems: Quantum stochastic differential equations and the master equation," *Phys. Rev. A*, vol. 31, pp. 3761–3774, Jun 1985.

[27] J. Zeiher, R. van Biijnen, P. Schauss, S. Hild, J. Choi, T. Pohl, I. Bloch, and C. Gross, "Many-body interferometry of a rydberg-dressed spin lattice," *arXiv:1602.06313*, 2016.